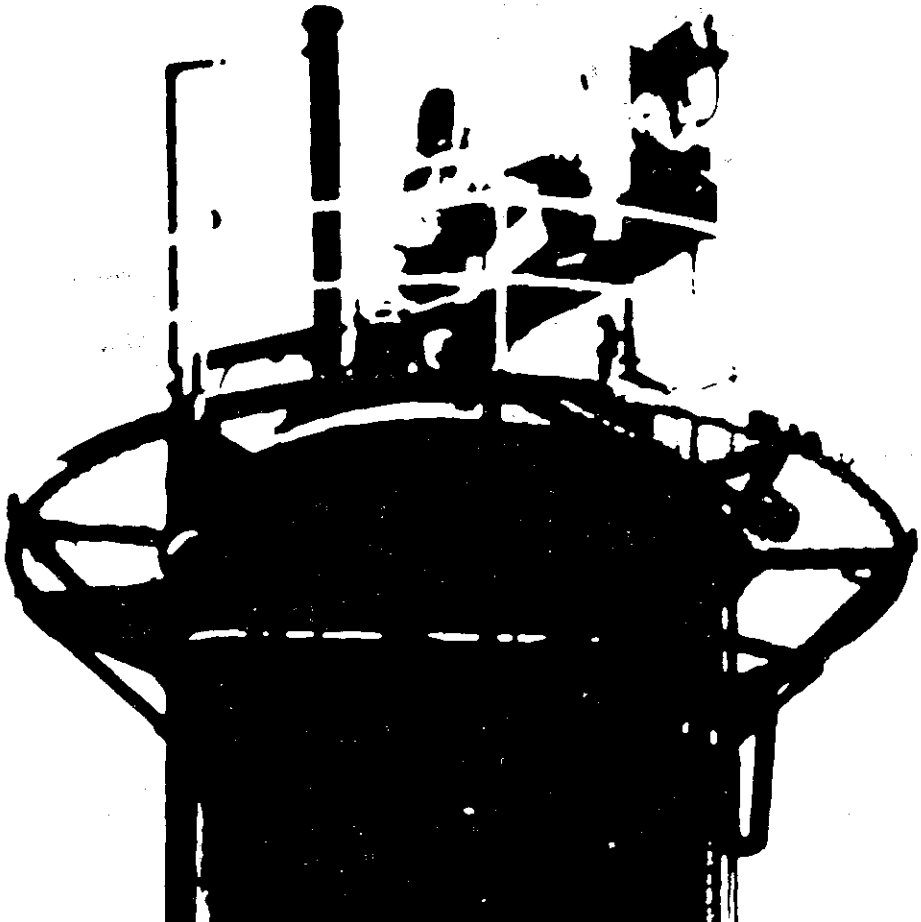

FIXED BED CATALYTIC REACTORS

The author discusses an improved two-dimensional model for reactions in fixed beds and illustrates its use with a relatively complex reaction system representative of commercial hydrocarbon oxidation

The design of fixed bed catalytic reactors of the tubular type has generally been based upon a one-dimensional model. In this model it is assumed that concentration and temperature gradients occur only in the axial direction, and that the only transport mechanism operating in this direction is the overall flow itself, considered to be of the plug flow type. In many cases, however, radial temperature gradients are inevitable.

The one-dimensional model, then, leads to average values for the temperatures and conversions and provides no information concerning excessive temperatures along the axis, which may be markedly different from the mean and unacceptable for reasons of reactor stability, process selectivity, and catalyst deactivation. This paper reports on an investigation of the reliability of the one-dimensional model. It is compared with a more elaborate two-dimensional model that takes the existence of radial gradients into account. The basic data required by this approach are reviewed. The reaction scheme considered is of a relatively complex nature and representative of commercial hydrocarbon oxidation.

ONE-DIMENSIONAL MODEL WITH PLUG FLOW

The equations describing nonisothermal, nonadiabatic, steady-state operation are well known. For a single reaction, $A \rightarrow B$, they may be written:

$$\frac{dx}{dz'} = \frac{\rho_b M_m}{N_{A_0} G} r_A$$

$$\frac{dt}{dz'} = \frac{(-\Delta H)}{Gc_p} r_A - \frac{4\,U}{Gc_p d_t} t$$

The integration of this system of ordinary differential equations is generally not feasible by analytical methods. Numerical integration on digital computers, however, presents no special difficulty. The analog computer is also eminently suited for integration of such systems.

One important aspect of design, particularly with exothermic reactions, is "stability" or "parametric sensitivity." With exothermic reactions, the tubular reactor generally experiences a temperature peak. The problem is to choose the steady-state inlet values of the parameters in such way that the hot spot does not become excessive, even when these inlet values are subject to perturbations. This sensitivity problem was first treated analytically by Bilous and Amundson (5). They considered the transient continuity and energy equations for the reactor, linearized them about the steady-state values at each point, and studied the effect of a sinusoidal input perturbation. Predictions of the

sensitivity are possible, provided one steady-state profile has been calculated. This annihilates much of the benefit of the approach; once the computer program has been written to calculate one steady-state profile, it is much easier to investigate the sensitivity by running the program a number of times for a set of values of the inlet parameters. This is what Barkelew has done for the single reaction A → B, with the aim of establishing a criterion for the parametric sensitivity (*1*). The results are shown in Figure 1.

N/S is the ratio of the rate of heat transfer per unit volume at $\tau = 1$, where $\tau = (E/RT_s^2)(T - T_s)$ to the rate of heat generation per unit volume at $\tau = 0$ and zero conversion—i.e., at the entrance. Ratio τ_{max}/S is that of the dimensionless maximum temperature to the adiabatic temperature rise above the coolant temperature. A set of curves is obtained, with S as parameter. The curves show an envelope occurring very near to the knee of an individual curve. Above the tangent to the envelope, τ_{max} changes rapidly with N/S, but not below the tangent. Barkelew's criterion concludes that the reactor is stable with respect to small fluctuations if its maximum temperature is below the value at the tangent to the envelope.

The criterion is conservative, not only because it is based upon an envelope, but also because the temperature dependence of the rate coefficient was forced, for the sake of convenience, into a form somewhat different from the Arrhenius law. Figure 2 compares the values of the excess temperatures derived from the above plot with those obtained by numerical integration. However, using the true rate equation according to Arrhenius, for the case of a single pseudo-first-order reaction, we have:

$A + P \rightarrow B$, with $\Delta H = -307$ kcal./gram mole,

$$\ln k = -\frac{13{,}636}{T} + 19.837$$

$\rho_b = 1300$ kg./cu. meter, $M_m = 29.48$, $N_{A_0} = 0.00927$

$N_{p_0} = 0.208$, $G = 4684$ kg./sq. meter hr., $c_p = 0.25$ kcal./kg. ° C.

$d_t = 0.025$ meter (curves 1 and 2)

Curve 3 has been obtained by an analytical procedure which linearizes the true rate equation around the inlet values

$$r = A' + B'x + C't$$

where $t = T - T_0$

This is the most general linear form retaining the coupling between the continuity and energy equations. For mild conditions the agreement is excellent.

To arrive at some prediction about the sensitivity, we do not have to go through the complete integration; the roots of the characteristic equation are obtained by Laplace transformation of the system of equations, and

CURRENT DESIGN STATUS

G. F. FROMENT

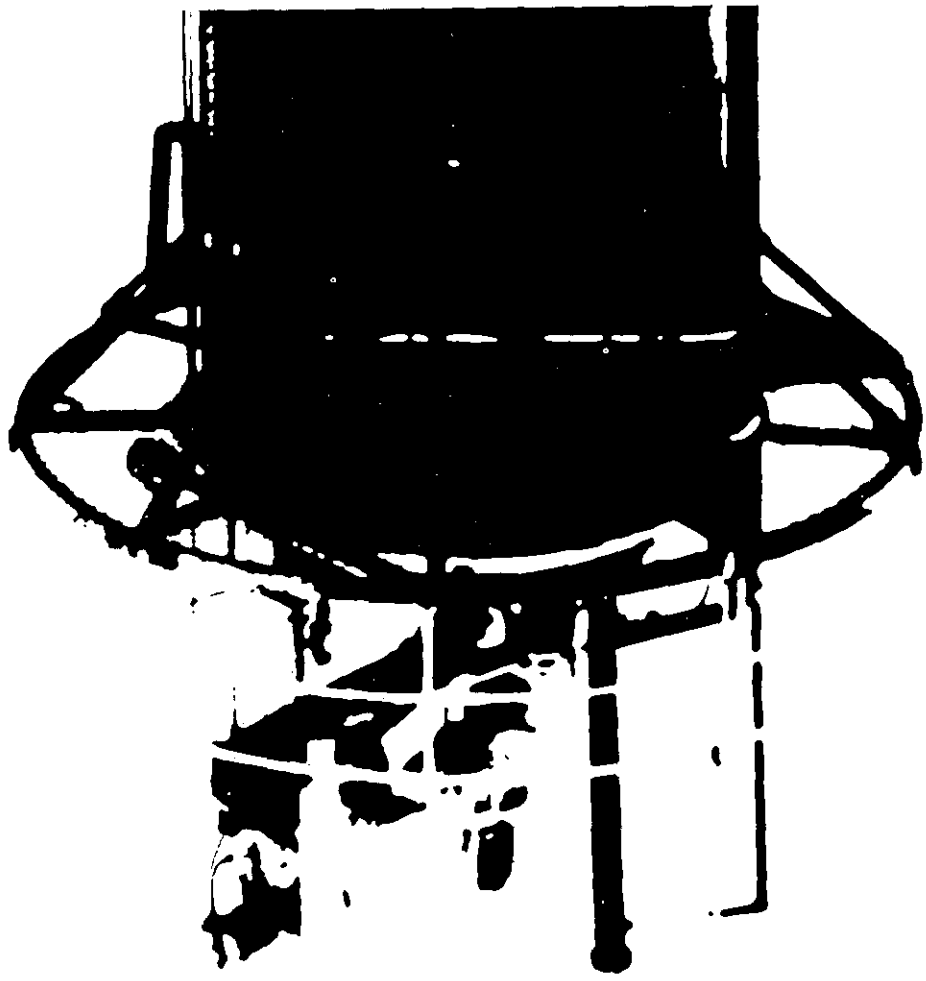

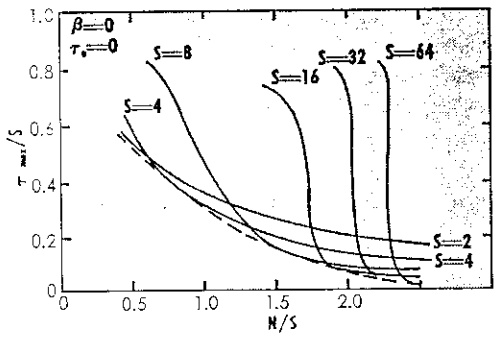

Figure 1. "Stability" criterion according to Barkelew (1)

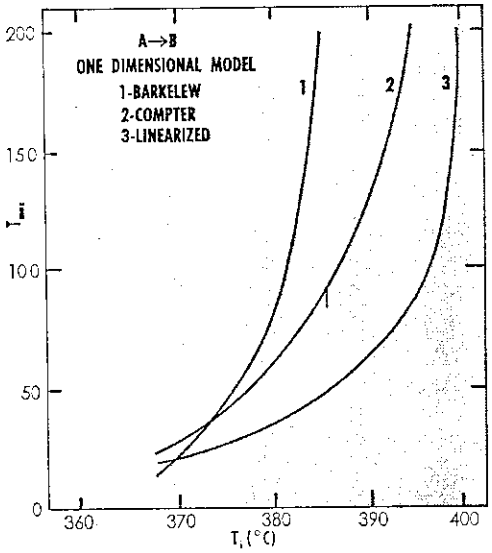

Figure 2. Maximum temperature as a function of inlet temperature

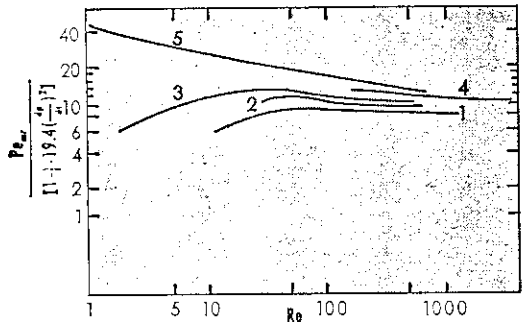

Figure 3. Radial effective diffusivity data: 1, Fahien and Smith (17); 2, Bernard and Wilhelm (4); 3, Dorrweiler and Fahien (15); 4, Plautz and Johnstone (33); 5, Hiby (22)

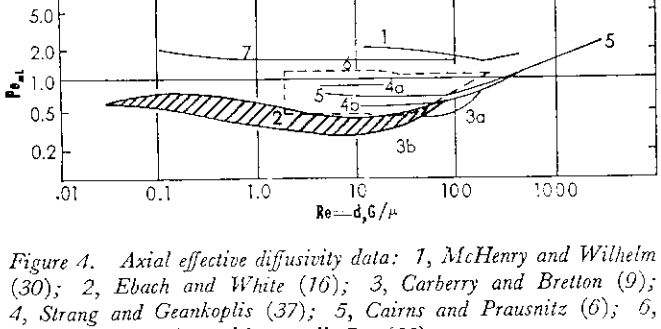

Figure 4. Axial effective diffusivity data: 1, McHenry and Wilhelm (30); 2, Ebach and White (16); 3, Carberry and Bretton (9); 4, Strang and Geankoplis (37); 5, Cairns and Prausnitz (6); 6, Hiby (22); 7, Hiby, without wall effect (22)

this is sufficient for our purpose. Indeed, when the roots are positive, the temperature rises out of bounds. We see that the treatment is completely analogous to the treatment of the stability of a continuous stirred tank. A slope condition at the entrance is found as criterion. As there is no feedback, any oscillatory behavior is introduced by the linearization. The runaway limit predicted in this way is in reasonable agreement with the results of the numerical integration. For the single reaction $A \rightarrow B$, carried out in a one-dimensional tubular reactor, a very wide spectrum of possible situations has been investigated by Barkelew. Evidently nothing like this is available for a complex reaction system, with its large number of parameters. Complex cases will probably always be handled individually. Let it be noted also that the limitations upon the validity of the analytical treatment with linearized rate law become more stringent for such cases.

Whereas Barkelew investigated the parametric sensitivity by considering only the steady state, Liu and Amundson focused their attention more upon the stability, *sensu stricto* (*27*, *28*, *38*, *39*). They were more concerned with determining if the profiles in an adiabatic reactor return to the original steady state after removal of a perturbation. Therefore, they numerically integrated the transient equations describing the state of both the fluid and solid along their characteristics. The stability was shown to depend upon the state of the individual particles. For a certain range of the variables, more than one steady state is possible. With each particle having only one steady state, unique temperature and conversion profiles are obtained. These profiles are stable; after removal of a pertubation the system returns to its original state. With particles having multiple steady states, the concentration and temperature profiles are nonunique and dependent upon the initial state of the bed. Large perturbations, after removal, may leave the reactor in an entirely different state. Liu, Aris, and Amundson also considered the nonadiabatic reactor (*22*, *28*, *38*, *39*).

It has been proposed to refine the one-dimensional model by adding a term taking axial mixing into account. This leads to a second-order differential equation. The most complete investigation of this model was carried out by Carberry and Wendel for the reaction $A \rightarrow B \rightarrow C$ (*10*). Inter- and intraparticle heat and mass transfer were also considered. The effect of axial mixing was found to be negligible unless one is dealing with extremely shallow beds. The gradients within the particle are of great importance. There are several objections to the one-dimensional model.

The first concerns the velocity profile, which is not flat, as was shown—e.g., by Schwartz and Smith (*34*). A second, and more serious, objection concerns the radial temperature profile. The temperature in a cross section of the reactor can only be uniform when the resistance to radial heat transfer is zero. This condition is evidently not fulfilled, owing to the poor conductivity of catalyst supports, so that radial gradients are inevitable in nonisothermal, nonadiabatic catalytic reactors. If it is thought excess temperatures at the axis

may have the detrimental effects mentioned previously, there is a need for design models, which permit the prediction of the detailed temperature, and conversion patterns in the reactor. Such design models are of two-dimensional nature. Depending upon the underlying concept they can be classified in two broad categories:

1. Those based upon the effective transport concept, in which all transport, except that by the overall flow, is treated as a diffusion- or conduction-like phenomenon. This is the approach used by Baron (*2*), Smith (*36*), Beek (*3*), Mickley and Letts (*32*), and Froment (*18*)
2. Those based upon the mixing cell concept, in which all transport, except that by the overall flow, is considered as resulting from a sequence of mixing events taking place in a two-dimensional network of cells with complete mixing

The first approach leads to a boundary value problem, and the second leads to an initial value problem. The mixing cell model was first applied to the two-dimensional case by Deans and Lapidus, who mainly described the computational aspects (*14*). It was further used by McGuire and Lapidus who studied in detail the stability of the two-dimensional case, to which they extended Shean-Lin Liu and Amundson's work (*27*). They focused their attention exclusively upon the rather special situation in which multiple steady states are possible for the particles. McGuire and Lapidus distinguished between the gas and solid temperature and took gradients within the particles into account. As they had to deal with the transient equations, the computational effort almost became prohibitive.

In what follows, an effective transport model is set up, and its application to a realistic case involving yield problems is discussed. Particular attention is given to the problem of parametric sensitivity. Simultaneously, some insight will be gained into the reliability of the one-dimensional model described above. Before this can be done, however, it may be useful to review briefly some aspects of heat and mass transfer in packed beds.

TWO-DIMENSIONAL MODEL FOR HEAT AND MASS TRANSFER IN PACKED BEDS

Mass Transfer in Packed Beds

The hydrodynamics of packed beds are so complex that it is practically impossible to describe them rigorously and, even if it were possible, the resulting equations would be so complex as to defy practical application. Faced with such a situation, the chemical engineer uses mathematical models to simulate the real behavior. The model most generally used today superimposes upon the transfer by the overall flow an additional transfer, the formulation of which is based upon the observation that the travel of a fluid element between two points in a packed bed is built up of a large number of random steps, owing to the random orientation of the passages between the packing.

The flux due to such a process may be described by a formula completely analogous to Fick's first law of diffusion. In the case of a packed bed, the proportionality constant in this law is called the effective diffusivity and is a function of both the flow conditions and the properties of the fluid. Since packed beds are not isotropic for this effective diffusion, two components, one in axial and one in radial direction, have been considered. When the fluxes due to effective diffusion are superimposed on the flux due to the overall flow, the following continuity equation is obtained for a component flowing at steady state through a cylindrical packed bed in the absence of reaction:

$$u(r) = \frac{\partial c}{\partial z'} = \frac{\partial}{\partial z'}\left[D_L'(r')\,\frac{\partial c}{\partial z'}\right] + \frac{1}{r'}\,\frac{\partial}{\partial r'}\left[D_R'(r')\,\frac{\partial c}{\partial r'}\right]$$

an equation which may be further simplified to

$$u\left(\frac{\partial c}{\partial z'}\right) = D_L\left(\frac{\partial^2 c}{\partial z'^2}\right) + \left(\frac{D_R}{r'}\right)\frac{\partial}{\partial r'}\left(r'\,\frac{\partial c}{\partial r'}\right)$$

where D_R is the mean of $D_R'(r')$. However, D_L differs from the mean of $D_L'(r')$ because of the effect of the velocity profile (*32*). The major part of the data available in the literature pertain to the class D_R and D_L. We will not discuss the methods for obtaining D_R and D_L from residence time distribution data, but we will briefly review the results which are of interest in the design of chemical reactors.

Radial Effective Diffusivity, D_R

The available data are brought together in a Pe_{mR} *vs.* Re diagram shown in Figure 3. Because of wall effects, the importance of which grows with increasing d_p/d_t, it is found that Pe_{mR} also depends on d_p/d_t. Dorrweiler and Fahien (*15*), and Fahien and Smith (*17*) correlated their data obtained at several values of d_p/d_t by using as an ordinate

$$Pe_{mR}/\left[1 + 19.4\left(\frac{d_p}{d_t}\right)^2\right]$$

rather than Pe_{mR} itself. It is to be noted that Hiby's experiments, free of wall effects, lead to higher Pe_{mR} (*22*).

In the laminar flow range the contribution of molecular diffusion is significant and Pe_{mR} depends on the properties of the fluid, expressed by the Schmidt number. In the turbulent flow range, however, D_R has been found to vary proportionally with the flow velocity so that Pe_{mR} becomes independent of Re. For practical applications we will note that Pe_{mR} lies between 8 and 11.

Axial Effective Diffusivity

The available data are shown in Figure 4, again in a Pe *vs.* Re diagram. The data, obtained by McHenry and Wilhelm for gases, indicate that Pe_{mL} is also independent of Re in the higher flow range (*30*). The

AUTHOR *G. F. Froment is Professor of Chemical Engineering at the Rijksuniversiteit, Ghent, Belgium.* *The author acknowledges the aid of W. Vanderleen and R. Van Welsenaere of the Rekenlaboratorium, Rijksuniversiteit, Ghent, in performing calculations for this paper.*

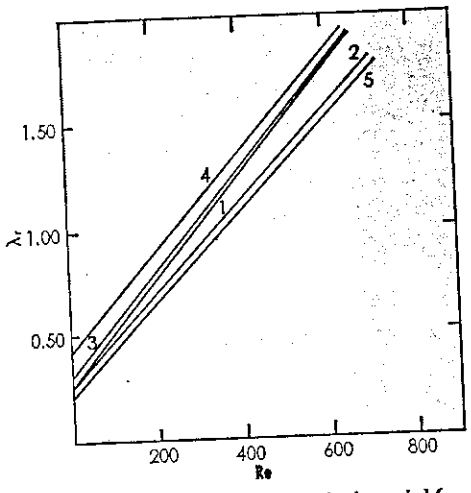

Figure 5. Effective thermal conductivity data: 1, Coberly and Marshall (11); 2, Campbell and Huntington (8); 3, Calderbank and Pogorsky (7); 4, Kwong and Smith (24); 5, Kunii and Smith (23)

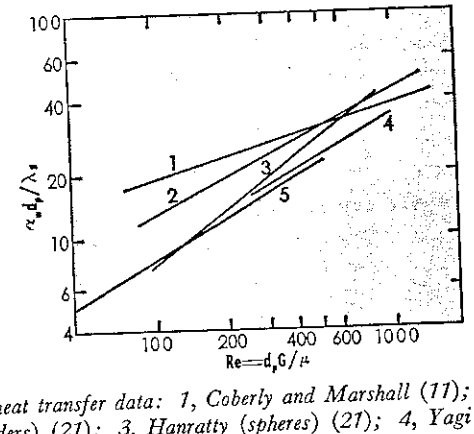

Figure 6. Wall heat transfer data: 1, Coberly and Marshall (11); 2, Hanratty (cylinders) (21); 3, Hanratty (spheres) (21); 4, Yagi and Wakao (43); 5, Yagi, Kunii, and Wakao (42)

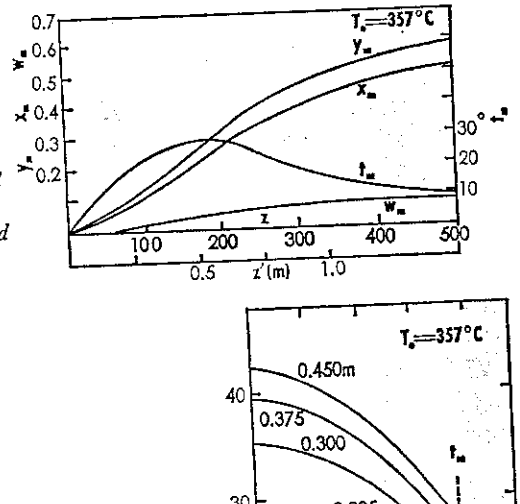

Figure 7. Radial mean conversions and temperature as functions of bed length

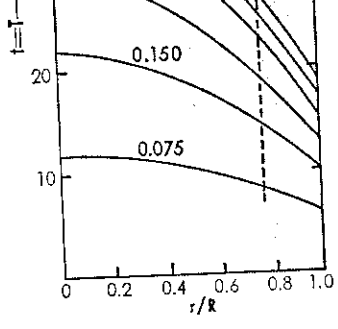

Figure 8. Radial profiles of temperatures at several bed lengths

data for liquids slowly tend toward those for gases. Hiby has measured D_L values that strongly depend on the velocity profile and short-circuiting effects. For design purposes Pe_{mL} may be considered to lie between 1 and 2.

Heat Transfer in Packed Beds

The transfer of heat in packed beds is even more complicated because of the participation of the solid phase and because of radiation effects.

The transfer is considered under two aspects: (1) convection by plug flow and (2) all the other effects. To describe the latter without complicating the design equations prohibitively, the bed, consisting of fluid and solid, is considered as a homogeneous body through which heat is transferred by effective conduction. This effective conduction is superimposed upon the overall convection, supposed to be of the plug flow type. A heat balance on a differential element in the steady state and in the absence of reaction then takes a form completely analogous to that of the continuity equation:

$$\lambda_R\left[\frac{\partial^2 t}{\partial r'^2}+\frac{1}{r'}\frac{\partial t}{\partial r'}\right]+\lambda_L\left[\frac{\partial^2 t}{\partial z'^2}\right]-G c_p\left[\frac{\partial t}{\partial z'}\right]=0$$

where the bed is considered to be anisotropic for "effective" conduction and λ_R, λ_L, and G are independent of the radial position. Yet, upon measuring λ_R experimentally, we see that it decreases considerably in the vicinity of the wall, probably because of variations in fluid properties, system geometries, and flow velocities. It is as if a supplementary resistance is experienced near the wall. Two alternatives are open: Either use a mean λ_R, or consider λ_R as a constant at the value in the central core and introduce a wall heat transfer coefficient, α_w, defined by:

$$\alpha_w(t_R-t_w)=-\lambda_R\left(\frac{\partial t}{\partial r'}\right)$$

When it is of importance to predict point values of the temperature with the greatest possible accuracy, the second approach is preferred.

Radial Effective Thermal Conductivity

Figure 5 shows some of the most reliable data obtained, until now, for λ_R. It is seen that λ_R varies linearly with Reynolds number. While the other lines were obtained or calculated for alumina or celite packing and air, the line representing Kwong and Smith's data gives an idea of the influence of the conductivity of the solid itself, in this case steel (24). Strictly speaking, these results are restricted to the conditions under which they were obtained. They provide no means for extrapolation to other conditions. This requires a model for heat transfer in packed beds.

The most elaborate model available today is that of Yagi and Kunii (40) and Kunii and Smith (23), but it goes back to pioneering work by Singer and Wilhelm (35). The model considers the heat flux by effective conduction as resulting from two contributions: one static, the other dynamic. The static contribution,

measured in the absence of flow, considers heat transferred in the fluid and the solid by conduction and radiation. The dynamic contribution may be predicted on the basis of data on effective radial diffusivity. The straight line numbered 5 in Figure 5 is calculated on the basis of this theoretical model for the mean conditions of the reported experiments. The agreement is quite satisfactory.

Wall Heat Transfer Coefficient

The available data are reviewed in Figure 6, which shows considerable scatter. Early correlations of the form $\alpha_w d_p/\lambda_g = mRe^n$ are only valid from a certain Re upward, since they would predict a zero value for α_w at Re = 0, which is not correct. Therefore, Yagi and Kunii proposed an equation of the type

$$\frac{\alpha_w d_p}{\lambda_g} = \frac{\alpha_w{}^0 d_p}{\lambda_g} + \Psi \mathrm{Pr}\,\mathrm{Re}$$

where $\alpha_w{}^0$ may be calculated on the basis of a model analogous to the one proposed for the static contribution to λ_R (*41*). It should be pointed out here that α_w is fundamentally different from the so-called "overall" heat transfer coefficients measured by Colburn (*12*), Leva (*25*), Maeda (*31*), and Verschoor and Schuit (*44*), which are based on mean temperatures in the bed, as if there were no radial gradients. It is as if there were no resistance to heat transfer in the central core. We will not enter into details about λ_L, the effective thermal conductivity in axial direction. In industrial reactors the flux due to axial effective conduction may be neglected compared to that due to the overall flow (*10*).

DESIGN OF FIXED BED CATALYTIC REACTORS BASED ON EFFECTIVE TRANSPORT MODELS

To date, a two-dimensional model for predicting temperature and concentration gradients in packed beds has been established, and the experimental data required for its application have been reviewed. The treatment can easily be extended to the fixed bed catalytic reactor by completing the continuity and energy equations with terms accounting for the reaction. This leads to a system of nonlinear second-order partial differential equations, the integration of which is not possible by analytical methods. Yet, if the rate equation is linearized to

$$r_A = A' + B'x + d't$$

an analytical, or at least a semianalytical, solution is possible (*18*). Such a solution has rendered excellent service as a check for the computer solution, as a starting solution for those cases where the temperatures of the feed and of the outside wall of the tubes are not equal (*18*), and for giving an insight into the behavior of the reactor. It should be used with circumspection, however, and, although it will reveal where severe radial gradients are to be expected, the values it will predict for such cases may be considerably in error.

There exists a graphical procedure for integration of the system with the true rate equation, proposed by Schmidt, and applied by Baron (*2*), but it is not sufficiently precise and is very tedious. Even for the digital computer, the numerical integration of a system of nonlinear, second-order, partial differential equations is a serious problem, for reasons of mathematical stability of the solution. J. Beek discussed this integration and carried it out for a reaction $A \rightarrow B$ and a set of typical values of the parameters (*3*). Mickley and Letts (*32*) used an implicit difference formulation but with explicit evaluation of nonlinear terms. They applied it to the reaction $A \rightarrow B \rightarrow C$ and calculated the influence of radial gradients on the yield. In Ghent, the implicit Crank-Nicholson procedure (*13*) has been adopted; the details have already been discussed (*20*). The program was tried out in 1961 and has since been applied to several cases.

The case considered here is of a rather complex nature, namely

This reaction model is fairly representative of the gas phase air oxidation of *o*-xylene into phthalic anhydride on V_2O_5 catalysts. *A* represents *o*-xylene, *B* phthalic anhydride, and *C* the final oxidation products to CO and CO_2.

Air is used in very large excess. The *o*-xylene mole fraction is generally kept below 1%, to stay under the explosion limit. One way of carrying out this very exothermic process is to use a multitubular reactor, consisting of 2500 tubes of 2.5 cm. diameter, 2.5 to 3 meters long, packed with catalyst and cooled by a salt bath that transfers the heat of reaction to a steam generator. Owing to the very large excess of oxygen, the rate equations may be considered, in first approximation, to be of the pseudo-first-order type, so that at atmospheric pressure:

$$r_A = (k_1 + k_3)N_{A_0} N_0 (1 - y)$$

$$r_B = N_{A_0} N_0 [k_1(1 - y) - k_2 x]$$

$$r_C = N_{A_0} N_0 [k_2 x + k_3(1 - y)]$$

with $y = x + w$

$$\ln k_1 = -\frac{27{,}000}{1.98\,(t + T_0)} + 19.837$$

$$\ln k_2 = -\frac{31{,}400}{1.98\,(t + T_0)} + 20.86$$

$$\ln k_3 = -\frac{28{,}600}{1.98\,(t + T_0)} + 18.97$$

When use is made of the following dimensionless variables,

$$z = \frac{z'}{d_p},\ r = \frac{r'}{d_p},\ t = T - T_0,\ R = \frac{R'}{d_p}$$

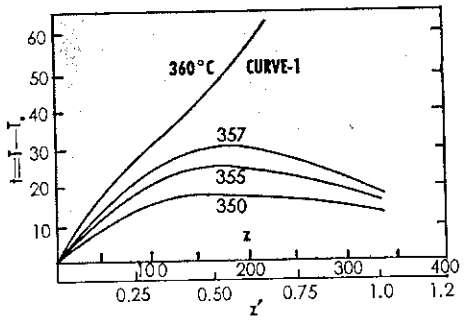

Figure 9. Radial mean temperatures as functions of bed length for several inlet temperatures

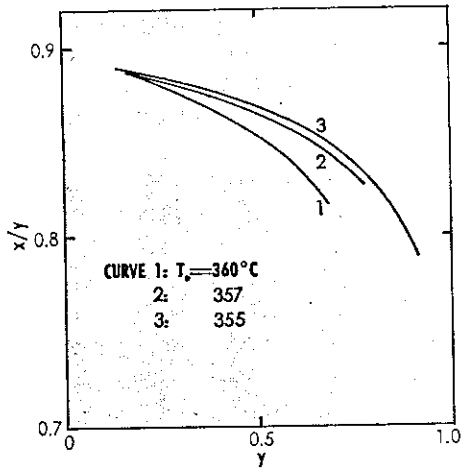

Figure 10. Outlet selectivity as a function of total conversion for several inlet temperatures

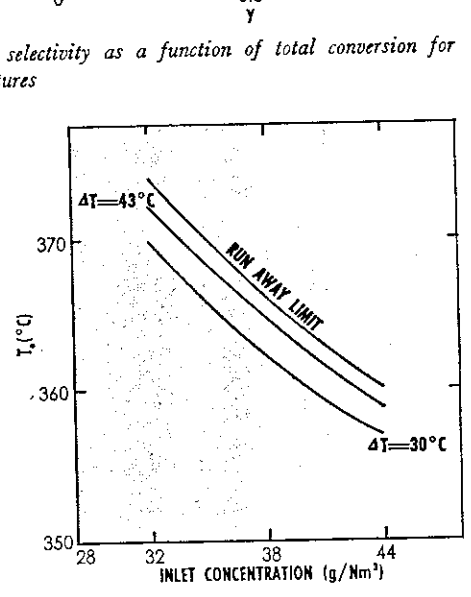

Figure 11. Effect of inlet concentration on runaway limit

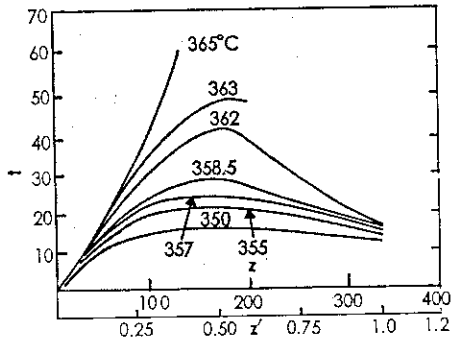

Figure 12. Temperature profiles for various inlet temperatures in a one-dimensional model

the steady-state continuity and energy equations may be written in cylindrical coordinates:

$$\left.\begin{aligned}\frac{\partial x}{\partial z} &= a_1\left(\frac{\partial^2 x}{\partial r^2}+\frac{1}{r}\frac{\partial x}{\partial r}\right)+b_1 r_B\\ \frac{\partial w}{\partial z} &= a_1\left(\frac{\partial^2 w}{\partial r^2}+\frac{1}{r}\frac{\partial w}{\partial r}\right)+b_1 r_C\\ \frac{\partial t}{\partial z} &= a_2\left(\frac{\partial^2 t}{\partial r^2}\right)+\frac{1}{r}\left(\frac{\partial t}{\partial r}\right)+b_2 r_B+b_3 r_C\end{aligned}\right\} \qquad (1)$$

Note that the term for axial effective transport was dropped in these equations. At the high flow rates used in practice, the contribution of this mechanism may be neglected. The constants in these equations have the following meaning:

$$a_1=\frac{D_R\rho_f}{G_t d_p}=\frac{1}{\mathrm{Pe}_{mR}} \qquad b_1=\frac{\rho_b d_p M_m}{GN_{A_0}}$$

$$a_2=\frac{\lambda_R}{Gc_p d_p}=\frac{1}{\mathrm{Pe}_{hR}} \qquad b_2=\frac{\rho_b d_p(-\Delta H_1)}{Gc_p}$$

$$b_3=\frac{\rho_b d_p(-\Delta H_3)}{Gc_p}$$

The boundary conditions are as follows:

$$x=0,\quad w=0 \qquad \text{at } z=0$$

$$\frac{\partial x}{\partial r}=0,\quad \frac{\partial w}{\partial r}=0 \qquad \text{at } r=0$$

$$t=0 \quad \text{at } r=R \text{ and } z=0 \quad 0\le r\le R$$

$$\frac{\partial t}{\partial r}=0 \quad \text{at } r=0$$

$$\left(\frac{\partial t}{\partial r}\right)_R=-\frac{\alpha_w d_p}{\lambda_R}t=-\alpha_t$$

In the last boundary condition the resistance of the tube wall itself and the outside wall resistance are neglected. Bulk mean values are obtained from:

$$\zeta_m=2\int_0^1 \zeta\frac{r}{R}d\left(\frac{r}{R}\right)$$

The following typical data were used in the calculations: $(N_{A_0})_0=0.00924$ which corresponds to 44 gram moles/cu. meter, $N_0=0.208$, $\Delta H_1=-307$ kcal./gram mole, a single value of $\Delta H_3=-1.090$ kcal./gram mole for the formation of CO and CO_2, $d_t=0.025$ meter, $d_p=0.003$ meter, $\rho_b=1300$ kg./cu. meter, $G=4.684$ kg./sq. meter hr. From Kunii and Smith's equation (*23*), it follows that Re = 121. $\lambda_R=0.67$ kcal./meter hr. ° C., from Yagi and Wakao's equation (*43*). $\alpha_w=134$ kcal./sq. meter hr. ° C., so that $\mathrm{Pe}_{hR}=5.25$, whereas $\mathrm{Pe}_{mR}=10$.

In all cases the feed inlet temperature equaled that of the salt bath. Figure 7 shows the results obtained for an inlet temperature of 357° C. The bulk mean conversions and temperatures are plotted as a function of reactor length. The conversion in phthalic anhydride tends to a maximum, which is not shown on the figure. This is typical for consecutive reaction systems.

Also typical for exothermic systems is the "hot spot," where t_m equals about 30° C. Even for this case, which is not particularly drastic, the radial temperature gradients are severe, as may be seen on Figure 8. The temperature in the axis is well above the mean. So much for the inlet temperature of 357° C., where a length of 3 meters is sufficient to reach the maximum in phthalic anhydride concentration. What happens when the temperature is raised by only 3° C. to overcome this is shown in Figure 9. The temperature rise goes out of control—a good example of "parametric sensitivity."

It should be remarked here that the upper part of Curve 1 may be considerably in error, because the heat transfer between gas and solid may become rate-controlling. To take this phenomenon into account would require the addition of equations to the system (*5*)—the effective transport concept does not distinguish between the gas and solid temperatures. There can be no doubt, however, about the existence of critical conditions for a feed temperature of 360° C. The "hot spot" experienced under these conditions, even less dramatic than shown in Figure 9, may be detrimental for the catalyst. Even if it were not important, "hot spots" would be unacceptable for reasons of selectivity. Indeed, the kinetic equations are such that the side reactions are favored by increasing the temperature. Just how detrimental the influence of the hot spot on the selectivity or yield is can be seen in Figure 10, in which the yield is plotted as a function of total conversion for several inlet temperatures. A few percentages more in yield, due to judicious design and operation, are important in high tonnage productions.

The inlet temperature is not the only parameter determining the runaway temperature. The influence of the hydrocarbon inlet concentration is shown in Figure 11, which summarizes Figure 9 obtained with 44 gram moles/cu. meter and two more diagrams like Figure 9, but obtained with 38 and 32 gram moles/cu. meter. Figure 11 shows how the runaway limit rises with decreasing hydrocarbon inlet concentration and the inlet temperatures which lead to hot spots of 43° and 30° C. It follows from the calculations leading to Figures 7 and 9, that, with 44 gram moles/cu. meter, an inlet temperature of 357° C. is insufficient to realize the desired conversion in the given length of 2.5 to 3 meters, while an inlet temperature of 360° C. causes runaway. Obviously, nobody would risk running the reactor within such narrow temperature limits.

If it is impossible to increase the bed length, the calculations show that for the range of inlet concentrations considered the hot spot has to exceed 30° C. That Figure 11 reveals operation within the region of extreme sensitivity is inevitable. No gain in safety margin is to be expected from a decrease in inlet concentration. Moreover, such a measure would decrease the production capacity and influence unfavorably the economics of the plant. With the given length there seems to be only one way out, that is to realize an entirely different type of temperature profile, showing no real hot spot, but leading all together to a higher average temperature. An appropriate dilution of the catalyst with inert packing in the early sections of the bed would make this possible.

COMPARISON OF RESULTS BASED ON ONE- AND TWO-DIMENSIONAL MODELS

For the one-dimensional model with plug flow the system of Equations 1 reduces to

$$\frac{dx}{dz} = b_1 r_B$$

$$\frac{dw}{dz} = b_1 r_C$$

$$\frac{dt}{dz} = -\frac{4\,U}{Gc_p d_t}\,t + b_2 r_B + b_3 r_C$$

The coefficient U is an "overall" heat transfer coefficient obtained under the assumption that the resistance to heat transfer is localized in a thin film near the wall (*12*, *25*, *29*). If the predictions based on the one-dimensional model are to be compared with those based on the two-dimensional model, it is necessary to use the same heat transfer data in both models. In other words, it is necessary to build up U from λ_R and α_w. This can be done in the following way (*18*): The temperature in a packed bed heat exchanger, in which there is no reaction, may be written, when the gradients are not accounted for, as

$$\bar{t}' = e^{-Kz} \quad \text{where} \quad \bar{t}' = \frac{T - T_0}{T_0 - T_s},\ K = \frac{4\,U}{Gc_p d_t}$$

but when the gradients are accounted for:

$$t'(r,z) = 2\,\alpha R \sum_{n=0}^{\infty} \frac{e^{-\left(\frac{a_2}{R^2}\lambda_n^2 z\right)}\, J_0\left(\lambda_n \frac{r}{R}\right)}{(\lambda_n^2 + \alpha^2 R^2) J_0(\lambda_n)}$$

Integration of this equation over the cross section leads to the values of $t_m'(z)$ that have to be compared with $t'(z)$:

$$t_m' = 2\int_0^1 t\,\frac{r}{R}\,d\left(\frac{r}{R}\right)$$

$$t_m' = 4\,\alpha^2 R^2 \sum_{n=0}^{\infty} \frac{e^{-\left(\frac{a_2}{R^2}\lambda_n^2 z\right)}}{\lambda_n^2(\lambda_n^2 + \alpha^2 R^2)}$$

If $\bar{t}'$ is to match closely t_m', the parameter K must be such that the exponential function $\bar{t}'(z)$ matches a sum of exponential functions. The value of K, to achieve this in the best possible way, may be obtained from the condition when the moments of zero order of both equations are equal. This leads to:

$$\frac{1}{K} = \frac{4\,\alpha^2 R^2}{a_2} \sum_{n=0}^{\infty} \frac{1}{\lambda_n^4(\lambda_n^2 + \alpha^2 R^2)}$$

from which (*27*, *28*, *38*, *39*):

$$K = \frac{2\,a_2}{R}\left(\frac{4\,\alpha}{\alpha R + 4}\right)$$

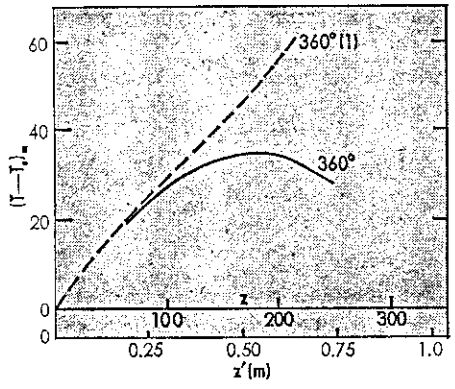

Figure 13. Influence of varying the effective thermal conductivity on the radial mean temperature profile

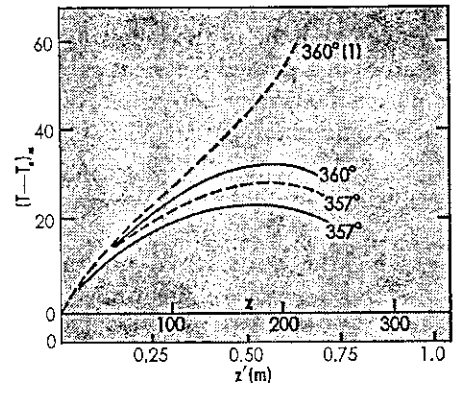

Figure 14. Influence of varying the wall heat transfer coefficient on the radial mean temperature profile

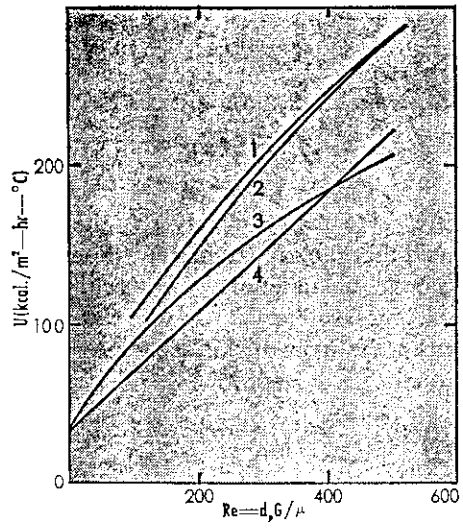

Figure 15. Comparison of overall heat transfer coefficient data: 1, Maeda (31); 2, Leva (25); 3, Verschoor and Schuit (44); 4, Yagi and Kunii (40, 41)

or finally

$$\frac{1}{U} = \frac{1}{\alpha_w} + \frac{R'}{4\,\lambda_R}$$

Using the λ_R and α_w correlations of Kunii and Smith (*23*) and Yagi and Wakao (*43*), previously used in the two-dimensional calculations, we are able to calculate U. That value is 82.7 kcal./sq. meter hr. ° C. and is used in the one-dimensional calculations shown in Figure 12, which is to be compared with Figure 9. The two-dimensional model predicts a runaway of the reactor for an inlet temperature of 360° C.

The one-dimensional model predicts a temperature rise of only 40° at an inlet temperature of 362° C., a rise of 48° at an inlet temperature of 363° C. The runaway temperature is now found to be 365° C. The discrepancy between the predictions of the one- and two-dimensional models grows as the hot spot increases in magnitude.

Some conclusions seem justified at this point. By its very essence, the one-dimensional model cannot provide any information about the detailed temperature and conversion pattern in the reactor. It was shown that, except for "mild" conditions, it may also fail to predict the mean temperatures and that the predicted values are always low for exothermic reactions. Yet, for practical purposes, the prediction of the runaway limit within five degrees of the two-dimensional model has to be considered excellent. Being much more tractable, the one-dimensional model will continue to be used for exploratory purposes and transient studies. The final calculations may be carried out on the basis of the two-dimensional model, particularly where considerable overtemperatures at the axis are to be feared for reasons of catalyst stability, process selectivity or, simply, safe operation. To date, the computer possibilities are such that the use of the two-dimensional model presents no difficulties when applied to the steady state.

There remains the question of how reliable our calculations, even those based on the most elaborate model, can be today. Their reliability depends, of course, on the value of the model itself and on the experimental parameters used in it. The next paragraph throws some light on the latter point.

INFLUENCE OF SOME OF THE PARAMETERS OF THE MODELS

The calculations for the two-dimensional model were repeated for several situations, drastic or not, but with $Pe_{mR} = 8$ instead of 10. The influence on the temperature and conversion profiles was completely negligible. It would, therefore, seem that our mixing data need not be refined further, at least for the usual situations. To get a feeling for the importance of the heat transfer parameters, calculations were performed with values of α_w and λ_e about 10% higher than those used in the calculations reported in Figure 9.

Figure 13 shows the temperature profile obtained for an inlet temperature of 360° C., but with $\lambda_e = 0.75$ kcal./meter hr. ° C., instead of 0.67, and with an un-

changed value for α_w of 134 kcal./sq. meter hr. ° C. The resulting overall coefficient U amounts to 86 kcal./sq. meter hr. ° C. instead of 82.7 for the reference curve "360" of Figure 9. The maximum mean overtemperature is now reduced to about 35° C.

Figure 14 shows the temperature profile obtained for the inlet temperature of 360° again, but with α_w = 150 kcal./sq. meter hr. ° C. instead of 134, and an unchanged λ_R of 0.67 kcal./meter hr. ° C. The corresponding overall coefficient is 88 kcal./sq. meter hr. ° C. Again, the radial mean temperature rise is reduced to about 35° C. Figure 14 also compares the curves obtained for a feed temperature of 357° C. The influence of α_w is less pronounced, of course, for this milder situation.

Variations in the values of the heat transfer coefficients of the order of 10% are well within the spread of the experimental results. This is illustrated by Figures 5 and 6 and for U by Figure 15, which compares overall coefficients built up from λ_R and α_w data of Kunii and Smith (*23*), and Yagi and Wakao (*43*), with these obtained by Leva (*25*), Maeda (*31*), and Verschoor and Schuit (*44*).

This figure clearly illustrates our continuing need for further research on heat transfer in packed beds. Heat transfer is not the only phenomenon of importance in the design of a chemical reactor, of course. We have given no attention to the influence of the rate of reaction. It is evident that the curves of Figure 9 could be shifted equally well by a slight modification of the kinetic coefficients of the rate equations.

It must be admitted the accurate prediction of critical situations like those encountered in the case considered requires a degree of precision in the measurement of the experimental parameters seldom achieved. Yet, even though the approach illustrated in this paper at least permits fixing limits between which the operating conditions in the industrial reactor have to lie, these limits are sufficiently narrow to make the final adjustments of relatively minor importance, so that neither the operating principle nor the expected results are affected by them.

NOMENCLATURE

A, B, C = chemical species
A', B', C' = constants in linearized rate equation
a_1 = reciprocal of Peclet number for effective radial mass transfer
a_2 = reciprocal of Peclet number for effective heat transfer
C = concentration
c_p = specific heat
D_L, D_R = effective diffusivities in axial and radial directions, respectively
D_L', D_R' = effective diffusivities in axial and point values, respectively
d_p = particle diameter
d_t = tube diameter
G = mass flow velocity, superficial
G_i = mass flow velocity, interstitial
ΔH = heat of reaction
k = rate coefficient
M_m = mean molecular weight
N_{A_0}, N_0 = inlet mole fraction of oxylene and oxygen, respectively
N_{P0} = inlet mole fraction of reactant p
r_A, r_B = rates of reaction
r' = radial coordinate
r = reduced radial coordinate = r'/d_p
R = radius
R' = reduced radius
t = temperature difference between reacting fluid and inlet or coolant temperature
T = absolute temperature
T_0 = temperature of feed and coolant, when equal
T_s = coolant temperature
U = overall heat transfer coefficient
u = linear interstitial velocity
w, x, y = conversions
z' = axial coordinate
z = reduced axial coordinate = $'/d_p$
α = $\alpha_w d_p/\lambda_R$
α_w = wall heat transfer coefficient
α_w^0 = wall heat transfer coefficient under static conditions
λ_L, λ_R = effective thermal conductivities, respectively, in axial and radial direction
λ_g = thermal conductivity of the gas
λ_n = set of positive roots of the transcendental equation $\chi J(\chi)/J_0(\chi) = \alpha_R$ where $J_0(\chi)$ and $J_1(\chi)$ are Bessel functions of the first kind, respectively, of zero and first order
K = $4\,U/Gc_pd_t$
ψ = a coefficient representative for the lateral mining near the wall
ρ_b = catalyst bulk density
$Pe_{hR}, Pe_{mL}, Pe_{mR}$ = Peclet numbers for effective transfer of heat and mass in axial and radial directions
Re = Reynolds number
Pr = Prandtl number
Nu = Nusselt number

REFERENCES

(1) Barkelew, C. R., *Chem. Eng. Prog. Symp. Ser.* **55** (25), 38 (1959).
(2) Baron, T., *Chem. Eng. Prog.* **48**, 118 (1952).
(3) Beek, T., "Advances in Chemical Engineering," pp. 3, 203, Academic Press, New York, 1962.
(4) Bernard, R. A., Wilhelm, R. H., *Chem. Eng. Prog.* **46**, 233 (1950).
(5) Bilous, O., Amundson, N. R., *Am. Inst. Chem. Eng. J.* **2**, 117 (1956).
(6) Cairns, E. J., Prausnitz, J. M., *Ibid.*, **6**, 400 (1960).
(7) Calderbank, P. H., Pogorsky, L. A., *Trans. Inst. Chem. Eng.* (*London*) **35**, 195 (1957).
(8) Campbell, T. M., Huntington, R. L., *Hydrocarbon Process. Petrol. Refiner*, **31**, 123 (1952).
(9) Carberry, J. J., Bretton, R. H., *Am. Inst. Chem. Eng. J.* **4**, 367 (1958).
(10) Carberry, J. J., Wendel, M., *Ibid.* **9**, 129 (1963).
(11) Coberly, C. A., Marshall, W. R., *Chem. Eng. Prog.* **47**, 141 (1951).
(12) Colburn, A. P., Ind. Eng. Chem. **23**, 190 (1951).
(13) Crank, G., Nicholson, P., *Proc. Camb. Phil. Soc.* **43**, 50 (1947).
(14) Deans, H. A., Lapidus, L., *Am. Inst. Chem. Eng. J.* **6**, 656 (1960).
(15) Dorrweiler, V. P., Fahien, R. W., *Ibid.*, **5**, 139 (1959).
(16) Ebach, E. A., White, R. R., *Ibid.*, **4**, 161 (1958).
(17) Fahien, R. W., Smith, J. M., *Ibid.*, **1**, 25 (1955).
(18) Froment, G. F., *Chem. Eng. Sci.* **7**, 29 (1961).
(19) Froment, G. F., *Gen. Chim.* **95**, 41 (1966).
(20) Grosjean, C. C., Froment, G. F., *Ned. Kon. Vl. Acad. Belg.* **24**, 1 (1962).
(21) Hanratty, T. J., *Chem. Eng. Sci.* **3**, 209 (1954).
(22) Hiby, W., Symp. on Interaction between Fruits and Particles, *Inst. Chem. Eng.* (London, 1962).
(23) Kunii, D., Smith, J. M., *Am. Inst. Chem. Eng. J.* **6**, 71 (1960).
(24) Kwong, S. S., Smith, J. M., Ind. Eng. Chem. **49**, 894 (1957).
(25) Leva, M., *Ibid.*, **40**, 747 (1948).
(26) Levenspiel, O., Bischoff K. B., "Advances in Chemical Engineering," p. 4, Academic Press, New York, 1963.
(27) Liu, Shean-Lin, Amundson, N. R., Ind. Eng. Chem. Fundamentals **1**, 200 (1962); **2**, 183 (1963).
(28) Liu, Shean-Lin, Aris, R., Amundson, N. R., *Ibid.*, p. 12.
(29) McGuire, M., Lapidus, L., *Am. Inst. Chem. Eng. J.* **11**, 85 (1965).
(30) McHenry, K. W., Wilhelm, R. H., *Ibid.*, **3**, 83 (1957).
(31) Maeda, S., *Tech. Rep. Tohoku Univ.* **16**, 1 (1952).
(32) Mickley, H. S., Letts, R. N., *Can. J. Chem. Eng.* **41**, 273 (1963); **42**, 21 (1964).
(33) Plautz, D. A., Johnstone, H. F., *Am. Inst. Chem. Eng. J.* **1**, 193 (1955).
(34) Schwartz, C. S., Smith, J. M., Ind. Eng. Chem. **45**, 1209 (1953).
(35) Singer, E., Wilhelm, R. H., *Chem. Eng. Prog.* **46**, 343 (1950).
(36) Smith, J. M., "Chemical Engineering Kinetics," McGraw-Hill, New York, 1956.
(37) Strang, D. A., Geankoplis, C. I., Ind. Eng. Chem. **50**, 1305 (1958).
(38) Wicke, E., Vortmeyer, D., *Z. Elektrochem.* **63**, 145 (1959).
(39) Wicke, E., *Ibid.*, **65**, 267 (1961).
(40) Yagi, S., Kunii, D., *Am. Inst. Chem. Inst. J.* **3**, 373 (1957).
(41) *Ibid.*, **6**, 97 (1960).
(42) Yagi, S., Kunii, D., Wakao, N., *Ibid.*, p. 543.
(43) Yagi, S., Wakao, N., *Ibid.*, **5**, 79 (1959).
(44) Verschoor, H., Schuit, G., *Appl. Sci. Res.* **A2**, 97 (1950).